What x rays can tell us about the interfacial profile of water near hydrophobic surfaces

Ahmet Uysal,[1,*] Miaoqi Chu,[1] Benjamin Stripe,[1,†] Amod Timalsina,[2] Sudeshna Chattopadhyay,[3] Christian M. Schlepütz,[4] Tobin J. Marks,[2] and Pulak Dutta[1]

[1]*Department of Physics and Astronomy, Northwestern University, Evanston, Illinois 60208, USA*

[2]*Department of Chemistry, Northwestern University, Evanston, Illinois 60208, USA*

[3]*School of Basic Sciences, Indian Institute of Technology Indore, Indore 452017, India*

[4]*X-Ray Science Division, Argonne National Laboratory, Argonne, Illinois 60439, USA*

(Received 13 March 2013; revised manuscript received 31 May 2013; published 17 July 2013)

The free surface of water and the interface between water and a hydrophobic surface both have positive interface energies. The water density near a free surface drops below the bulk density, and thus it is expected that water near a hydrophobic surface will also show a density depletion. However, efforts by multiple groups to detect and characterize the predicted gap at water-hydrophobic interfaces have produced contradictory results. We have studied the interface between water and fluoroalkylsilane self-assembled monolayers using specular x-ray reflectivity and analyzed the parameter-space landscapes of the merit functions being minimized by data fitting. This analysis yields a better understanding of confidence intervals than the customary process of reporting a unique best fit. We conclude that there are unambiguous gaps at water-hydrophobic interfaces when the hydrophobic monolayer is more densely packed.

DOI: 10.1103/PhysRevB.88.035431 PACS number(s): 61.25.Em, 68.08.−p, 82.70.Uv

I. INTRODUCTION

In traditional hydrodynamics, the liquid phase is generally treated as a uniform, structureless continuum. This assumption certainly fails at the free surface, where it is known that the density changes continuously rather than sharply from the bulk to the vapor, resulting in an intermediate-density surface region. It has long been suggested[1] that the interface between water and hydrophobic materials should be similar to the free surface of water, since both have positive surface tension. This analogy predicts that the water density near the hydrophobic substrate should drop below the bulk density, just as it does at the free surface, creating a density-depleted interfacial region. There may even be capillary fluctuations at this interface.[2–4] Such a depletion has also been invoked to explain the unusually large slip lengths seen in studies of shear flow at hydrophobic surfaces.[5]

In addition to the fundamental condensed-matter interest in the nature of the interfacial fluid phase, hydrophobic surfaces are common in nature; therefore, the structure and properties of water near hydrophobic surfaces are important in a large variety of applied contexts. Understanding the behavior of interfacial water is crucial, for example, to predicting the behavior of molecules such as proteins in aqueous environments, to modeling wet chemical reactions at interfaces, and to making water flow more easily in, e.g., lab-on-a-chip applications.

X-ray and neutron reflectivity have been extensively used to determine the density profiles at the free surfaces of many liquids,[6–25] including water,[22,25] and also at liquid-solid[26–28] and liquid-liquid[29,30] interfaces. These probes are sensitive to electron density and scattering length density, respectively, and for a known material, these are both measures of the local mass density. There is simply no other technique that so directly measures interfacial density profiles with the spatial resolution necessary for such studies. It is therefore natural to expect that x-ray and neutron reflectivity data will be equally informative at the water-hydrophobic interface and will give us unambiguous measurements of both time-averaged density profiles and of any capillary-wavelike dynamics at the interface.

In reality, although the water-hydrophobic interface has been studied by a number of groups,[30–37] the results are inconsistent and have not led to a consensus. Early neutron reflectivity studies[31–33] of hydrocarbon-water interfaces reported gap widths larger than 10 Å, while later x-ray reflectivity measurements on similar systems reported gap widths of less than 5 Å.[35,36] Yet, other x-ray[30] and neutron[34] studies reported that there is no gap. In retrospect, several major experimental obstacles can be identified:

First, reflectivity measurements have a finite spatial resolution[38] that depends on the inverse of the maximum momentum transfer reached in the reflectivity scan ($q_{\max}$). Convolution with the resolution function smears the effect being observed, both broadening and weakening it. Neutron reflectivity, in particular, covers a smaller q range because of the lower usable intensity; therefore, the resolution is relatively poor.[39]

Second, x-ray reflectivity is not chemically sensitive, so the interfacial density profile of the hydrophobic substrate, which is not of specific interest here, affects the reflectivity and obscures the profile of interest (that of interfacial water). This experimental difficulty does not exist at the air-water interface to which the water-hydrophobic interface is theoretically compared, since air has negligible electron density. Substrate roughness, for example, smears the interface profile. Silicon can be polished to 2–5-Å rms roughness, which is low compared with most other substrates, and silane-terminated molecules can easily be deposited on silicon to form very uniform hydrophobic self-assembled monolayers (SAMs). Thus, silicon-supported SAMs provide excellent, well-defined hydrophobic surfaces that have been used in many experimental studies.[31–33,35–37] However, there is a high price: the system now contains at least three interfaces, namely, silicon-oxide, oxide-SAM, and SAM-water. Only the last of

these is of interest here, but all interfaces reflect x-rays or neutrons and must be accounted for during data analysis.

Third, the reflectivity data must be fitted using model density profiles with adjustable parameters. The fitting procedure seeks to minimize the variance or other appropriate merit function by varying the model parameters, and it is customary to use fitting software to determine and report a best fit. This works well in those special cases where there is a unique and prominent minimum in the merit function. However, reflectivity data have finite range and significant error bars, and when fitted using a large number of parameters, the merit function landscape will often be quite complex.[40] There can be multiple local minima whose merit functions are not significantly different or continuous ranges of minima (referred to below as "valleys"). As noted previously, the hydrophobic surfaces that are otherwise ideal for x-ray studies (SAMs) contain at least three interfaces; therefore, fitting the reflectivity data requires many variable parameters (most of which are of no particular interest to us). In these circumstances, canned fitting software will still converge on a single best fit, but the appearance of certainty is deceptive. Worse, in pathological cases (see below), the best fit requires unphysical parameter values.

We have sought to address these three problems as follows. First, it has been previously shown[39] that increasing the hydrophobicity by using fluorocarbon-based SAMs is a good way to enhance the gap relative to the resolution limit. Reference 39 was limited to two different SAMs; in this paper we have added two more types of fluorocarbon SAMs to our study to see more clearly whether the interfacial gap width depends on monolayer properties. (Indeed, our studies do systematic comparisons rather than drawing general conclusions from a single system.) Second, while it is not currently possible to create a hydrophobic interface whose density profile is a single ideal step function, in this study we have used Si substrates with macroscopically thick layers of thermal oxide (formed by heating) rather than the more common ultrathin layers of native oxide (formed upon exposure to ambient oxygen at room temperature). This reduces the number of relevant interfaces by one, since the Si-SiO_2 interface is now buried too far below the surface for any coherent scattering to come from it. (The density contrast across the Si-SiO_2 interface is very small, and so its effect on real experimental data is slight. However, if incorrectly modeled, it can have a strong adverse influence on data fitting, as discussed below.) Third, in order to address the problem of multiple minima in the merit function landscapes, we have explored in some detail these landscapes and the effects of possible ways of fitting the same data. This provides a more informative and nuanced view of the fitting process, and a better understanding of what conclusions can and cannot be reliably drawn from these experiments and subsequent data analysis.

II. METHODS

Silicon substrates with ∼3000-Å-thick thermally grown layers of SiO_2 were obtained from WRS Materials. For the purposes of our experiment, these substrates can be treated as semi-infinite slabs of SiO_2. SAMs were deposited on the oxide surfaces using molecules with the general formula $CF_3(CF_2)_{(n-3)/2}(CH_2)_2SiCl_3$. These fluoroalkylsilane molecules will be referred to in the rest of this paper as FASn, where the number n is the total number of F atoms in each molecule. FAS13 (1H,1H,2H,2H-perfluorooctyltrichlorosilane) was purchased from Sigma Aldrich; FAS17 (1H,1H,2H,2H-perfluorodecyltrichlorosilane), FAS21 (1H,1H,2H,2H-perfluorododecyltrichlorosilane), and FAS25 (1H,1H,2H,2H-perfluorotetradecyltrichlorosilane) were purchased from Synquest Inc. Only FAS13 and FAS25, deposited on thin (native) silicon oxide, had been studied at the time of the initial report.[39] In the present study, all four types of molecules were self-assembled on thick oxide surfaces using the following procedure.[41] The substrates were cleaned by sonication in acetone and ethanol baths and were treated with oxygen plasma for 1 min. In moisture-free, nitrogen environments, 1-mM solutions of the fluorinated molecules were prepared in a 70/30 vol./vol. mixture of anhydrous isooctane and anhydrous carbon tetrachloride (Sigma Aldrich). Substrates were immersed in these solutions for 1–2 h at room temperature and finally rinsed with anhydrous solvents and ethanol.

The x-ray studies were conducted at Beamline 33-BM-C of the Advanced Photon Source, Argonne National Laboratory. The thin film cell used to hold SAM substrates and water was described in Ref. 39. The x-ray energy was 19 KeV (λ = 0.65 ˚A), and the beam was focused to 0.5 mm vertically and 2 mm horizontally. The data were collected with a Pilatus area detector. The off-specular background was determined simultaneously from the area detector by collecting counts in directions shifted $+0.2^\circ$ and -0.2° from the specular direction and averaging them. This background was subtracted from the specular counts.

The x-ray reflectivity $R(q)$ calculated from any electron density profile $\rho(z)$ is[42]

$$R(q) = R_F(q)\left|\frac{1}{\Delta\rho}\int\frac{d\rho(z)}{dz}e^{-iz\sqrt{q(q^2-q_c^2)^{1/2}}}dz\right|^2. \quad (1)$$

Here, R_F is the Fresnel reflectivity from a single ideal step-function interface, q_c is the momentum transfer at the critical angle for total external reflection, and $\Delta\rho$ is the total change in electron density across the interface (for example, when the surface is in contact with water, $\Delta\rho$ is the difference between SiO_2 and water electron densities). While this equation can be used to calculate $R(q)$ from a given analytic function $\rho(z)$, the reverse is not simple: when $R(q)$ is experimental data collected over a finite range and with finite accuracy, $\rho(z)$ cannot be directly calculated from it. Analysis of reflectivity data generally follows the same general procedures as all inverse problems: a model $\rho(z)$ is assumed, and parameters in the model are adjusted until good fits to the data are obtained.

Following the Parratt formalism (Ref. 43 and e.g., 44), a slab model was used to fit our data. In other words, the electron density profile $\rho(z)$ was represented by a series of segments with uniform density, except at the interfaces between slabs that are broadened by error functions:

$$\rho(z) = \rho_o + \sum_{i=0}^{n}\frac{\rho_{i+1}-\rho_i}{2}\left[1+erf\left(\frac{z-z_i}{\sqrt{2}\sigma_i}\right)\right]. \quad (2)$$

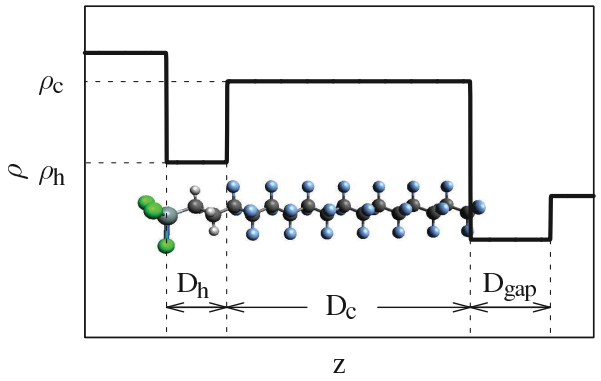

FIG. 1. (Color online) Schematic diagram of a fluoroalkylsilane molecule and a representation of the slab model of its density. The semi-infinite SiO_2 is at far left, and the semi-infinite water layer is at far right.

Here, ρ_o is the electron density of the semi-infinite substrate, ρ_i is the uniform density of the ith slab, and σ_i is the width of the interface between the $(i+1)^{\text{th}}$ and ith slabs.

Figure 1 shows a schematic diagram of the slabs used to describe the SAM (and the water profile, if any) and defines some of the parameters used. The semi-infinite SiO_2 layer is at far left (surface roughness σ_s). The molecule consists of a silane group that attaches to the SiO_2 surface, and two methylene (CH_2) groups, followed by a fluoroalkyl chain. A single slab (slab thickness D_h, electron density ρ_h, top surface roughness σ_h) was used to describe the combined silane and methylene groups, since the separation between them is much less than the resolution of the x-ray reflectivity technique. Another slab (thickness D_c, electron density ρ_c, and top surface roughness σ_c) was used for the fluorocarbon chain. When water is present, there is potentially an intervening gap (thickness D_{gap}, electron density ρ_{gap}, and top surface roughness σ_{gap}) followed by semi-infinite water (at far right in the diagram).

Minimizing $N^{-1}\sum_n [R_{\text{calc}}(q_i) - R_{\text{data}}(q_i)]^2$ does not work well with reflectivity data, because the reflectivity drops rapidly with q (roughly as $1/q^4$), which means that the variance is dominated by the largest (lowest q) numbers. The error-weighted function $\chi^2 \equiv N^{-1}\sum_n [R_{\text{calc}}(q_i) - R_{\text{data}}(q_i)]^2/\sigma_i^2$, where σ_i is the variance of the ith data point, works better but has been shown[45] to yield poor data fits at high q. We use instead the merit function

$$\gamma^2 \equiv N^{-1}\sum_n [\log R_{\text{calc}}(q_i) - \log R_{\text{data}}(q_i)]^2, \qquad (3)$$

which provides a more balanced weighting of the data over the entire q range.[45] To find the best fits, we employed the simulated annealing method[46,47] due to its simplicity and ability to avoid local minima.

III. RESULTS

A. Dry SAM studies

Determining the interfacial profile of the SiO_2-supported SAM (the dry interface) is not in itself a goal of this study. However, before we can study the substrate-water interface, it is essential to characterize the substrate and to better understand how fitting results must be evaluated.

Figure 2 shows reflectivity data and fits to characterize a dry SAM of FAS25 on silicon with thick (thermal) oxide. The best-fit parameters are listed in Table I. It should be noted that the density of a close-packed fluoroalkyl monolayer is quite high, about 80% of the substrate density. Thus, the electron density has one large step and one small step. This is in contrast to the more commonly studied alkylsilane SAMs, where the density is roughly half that of silicon, resulting in two roughly equal density steps.

Figure 2(a) and Table I illustrate the customary approach to the analysis of reflectivity data: a unique answer is presented based on the output of fitting software designed to minimize the appropriate merit function. To demonstrate that reality is more complex, Fig. 2(b) shows the γ^2 landscape in the D_c-ρ_c plane. For this calculation only, a simplified model was used with no head group slab ($D_h = 0$); in other words, the entire molecule is described by one slab. As the slab width (D_c) and density (ρ_c) are varied, it can be seen that there are not one but two minima in the merit function, and the customary fitting procedure might report either one of them. Both minima have the same D_c, but quite different ρ_c. In this case, it is not difficult to see why this happens. There are two interfaces in the electron density: first from air to the SAM and second from the SAM to the substrate. However, x rays cannot distinguish a small step followed by a big step (implying low SAM density) and from a big step followed by a small step (implying high SAM density). Indeed, it can easily be verified that the sum of the two best-fit values of ρ_c in Fig. 2(b) equals the known electron density of the silicon oxide substrate (1.9×10^{-5} Å^{-2}).

In other words, fitting programs cannot distinguish between the correct minimum and the wrong one; intelligent intervention is required. One can resolve the ambiguity here by estimating the electron density of a monolayer of fluoroalkylsilanes; this matches the higher value of ρ_c in Fig. 2(b).

TABLE I. Best-fit parameters for dry hydrophobic SAMs, with subscripts s = substrate (semi-infinite slab); h = head group slab; c = chain slab (see Fig. 1).

	From molecular model		Best fits to x-ray reflectivity data						
SAM	D_c (Å)	D_h (Å)	D_c (Å)	D_h (Å)	ρ_c (10^{-5} Å^2)	ρ_h (10^{-5} Å^2)	σ_c (Å)	σ_h (Å)	σ_s (Å)
FAS25	16.3	4.2	16.3	4.6	1.71	1.20	3.1	6.6	1.9
FAS21	13.8	4.2	13.6	4.5	1.75	1.00	3.0	6.9	2.7
FAS17	11.3	4.2	11.1	4.4	1.71	1.00	2.8	6.0	2.7
FAS13	8.8	4.2	8.5	4.4	1.50	1.23	3.0	6.1	1.7

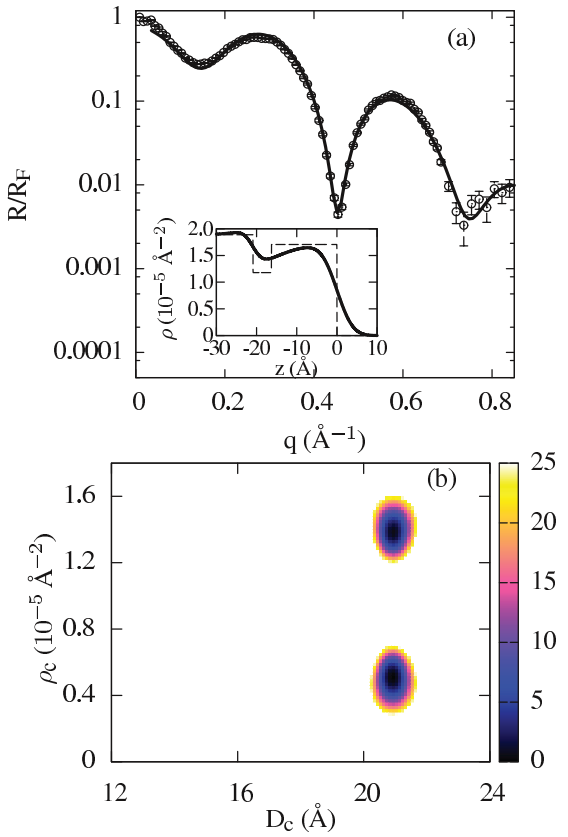

FIG. 2. (Color online) (a) Reflectivity data (open circles), best fit (solid line), and density profile (inset) for the dry FAS25 monolayer. The dashed line in the inset shows the density profile if the interfaces were not rounded, i.e., it shows the slabs more clearly (cf. Fig. 1). (b) Merit function landscape in the D_c-ρ_c plane (with $D_h = 0$ for simplicity). The merit function has been scaled and its minimum value subtracted in order to more clearly display the contours.

The additional information allows us to reject the lower SAM density solution as spurious. While this is a particularly simple example, it illustrates a general principle: reflectivity data analysis is almost always an ill-posed inverse problem (e.g., Ref. 48) and so judgment must always be exercised (and information from independent sources considered) in order to avoid choosing the wrong local minimum of the merit function.

A more interesting and subtle object lesson is provided in a recent paper[49] in which data from Ref. 39 were refitted to obtain an alternate density profile. That proposed density profile gave a good fit to the data, but only because the width of the Si/SiO_2 interface was assumed[50] to be 0.5 Å. This is not reasonable; such a picoscale model interface width predicts strong oscillations in the calculated reflectivity[50] that are not seen in reality from any clean Si substrates with native oxide. The Si/SiO_2 interface has been extensively studied not only with x rays[40] but also with transmission electron microscopy (e.g., Ref. 51) and is known to be at least 2–5 Å wide for the best-polished samples. When one fitting parameter is far from any realistic value, all other parameters required to force a fit to the data with this incorrect assumption will be incorrect also. Just as in our previous example, the existence of a good fit does not establish that it represents objective reality; it must still pass the additional tests of credibility and consistency with existing knowledge.

Indeed, throughout the x-ray reflectivity literature, the Si/SiO_2 interface is frequently used as a source of free parameters to improve the fits. The interface width varies from sample to sample, and its direct measurement is difficult so that any reasonable value may be assumed. In the present work, by using a thick thermal oxide as our substrate, we have removed this variability and reduced the number of free parameters available to us. The result is an improvement in the reliability of the fitting process. Further, in all the fits reported in the rest of this paper, we have excluded parameter ranges that are unrealistic. This is a long-established approach to solving ill-posed inverse problems.[48]

B. Water-SAM interface

Reflectivity data from the four SAMs of different chain lengths, now in contact with water, are shown in Fig. 3, and the corresponding best-fit parameters, including gap parameters (D_{gap}, ρ_{gap}), are listed in Table II.

It should be emphasized here that describing the gap as a single slab of uniform density and specific thickness, as illustrated in Fig. 1, is not meant to imply that the density depletion has that exact form in reality. Rather, it is an acknowledgment of the limited resolution available to experimentalists. An analogy may be made to pixelation in digital photographs: the gap is described by a single uniform-density slab only because a more complex description requiring more variable parameters is not justified by the information contained in the data. The gap widths and densities reported in this paper are merely effective widths and densities applicable to the single-pixel model of the gap. Theoretical calculations do report much more complex interfacial profiles,

TABLE II. Best-fit parameters for hydrophobic SAMs in contact with water, with subscripts s = substrate (semi-infinite slab), h = head group slab, and c = chain slab (see Fig. 1). ${\gamma_{min}}^2$ is the value of the merit function [Eq. (3)] for the fit. Note that, as shown in Figs. 4 and 5, many other sets of parameters give functionally equivalent fits, with merit functions comparable to the best fits. Thus, this table is not the full picture.

SAM	D_{gap} (Å)	ρ_{gap} (10^{-5} Å^2)	D_c (Å)	D_h (Å)	ρ_c (10^{-5} Å^2)	ρ_h (10^{-5} Å^2)	σ_{gap} (Å)	σ_c (Å)	σ_h (Å)	σ_s (Å)	${\gamma_{min}}^2$
FAS25	5.9	0.75	15.4	4.1	1.75	1.12	1.1	3.0	4.0	3.0	0.00207
FAS21	6.4	0.83	12.6	3.6	1.80	0.94	1.0	3.8	4.3	2.5	0.00103
FAS17	4.7	0.46	10.3	4.1	1.80	1.08	2.2	4.5	2.5	2.7	0.00228
FAS13	3.3	0.56	9.2	3.8	1.43	1.19	1.5	3.6	1.3	4.2	0.00621

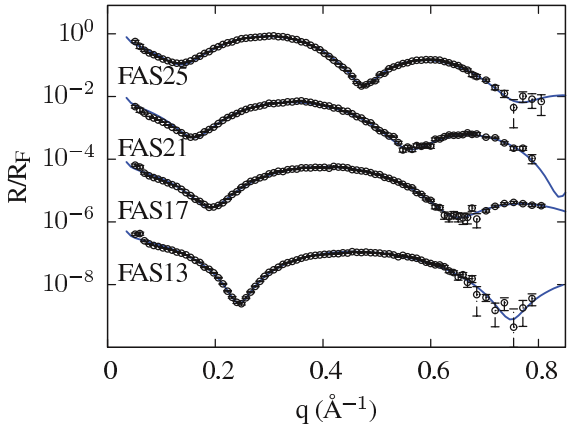

FIG. 3. (Color online) Reflectivity data (open circles) and best fits (solid lines), for SAMs of FAS13, FAS17, FAS21, and FAS25 in contact with water. The best-fit parameters are given in Table II.

but currently there are no experimental tools that can verify the finer details of these predictions.

Figure 4(a) shows the density profile for wet FAS25 that gave the best fit to the reflectivity data using physically feasible parameters (Fig. 3). Figures 4(b)–4(c) show contours illustrating the dependence of γ^2 on the gap width D_{gap} and gap density ρ_{gap}. The y axes of the contour plots are the relative depth of the gap rather than its density, i.e., $(\rho_{\text{water}} - \rho_{\text{gap}})/\rho_{\text{water}}$, since this is more intuitive: 0.0 means there is no gap, and 1.0 corresponds to the maximum possible depth (zero density). Fits were also done into the region $\rho_{\text{water}} < \rho_{\text{gap}}$ (negative y axis) in order to see if an "inverted gap" (density enhancement) might also fit the data.

The first contour, Fig. 4(b), is obtained as follows: all parameters other than D_{gap} and ρ_{gap} are fixed at their global best-fit values, while the gap parameters are allowed to vary. In this case there is a clear, well-localized minimum of γ^2; the width of the gap is ~6 Å, more than twice the size of a water molecule. While such constrained fits are sometimes reported, the appearance of precision is very deceptive. In Fig. 4(c) the merit function is minimized at each point in this plane, while allowing all parameters (including SAM density, thickness, etc.) to vary as much as 10% from the best-fit values. Under these conditions, the γ^2 landscape does not have a localized minimum. Rather, there is now a long "valley," which means that a variety of combinations of gap width and depth will produce good fits to the data.

The dashed line in Fig. 4(c) is the curve of constant "equivalent width":

$$D_{\text{eq}} \equiv D_{\text{gap}}(\rho_{\text{water}} - \rho_{\text{gap}})/\rho_{\text{water}}. \quad (4)$$

This is the width of a gap with the same integrated density depletion but with zero gap density (maximum depth). Along the dotted line, D_{eq} is constant and equal to its value at the best fit. It has previously been suggested[36] that x rays are more sensitive to the integrated depletion. If D_{eq} were the same for all best fits, the merit function minimum would be spread out in a curved "valley" following the dashed line. While that is not precisely the case here, the shape of the valley is somewhat similar to the constant D_{eq} line.

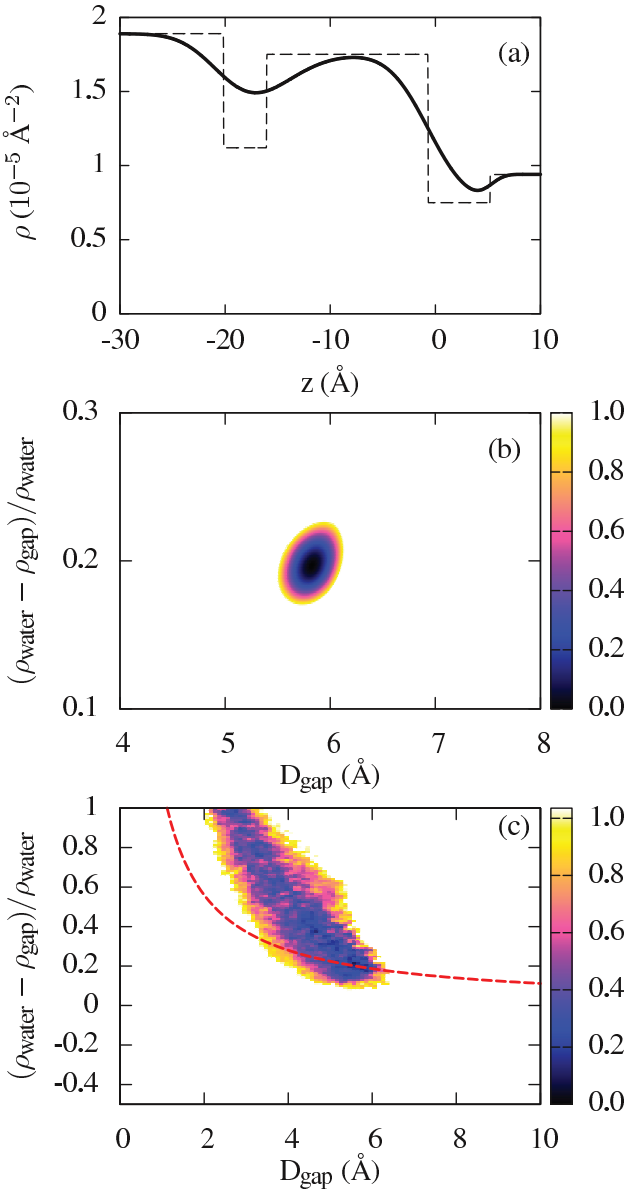

FIG. 4. (Color online) Fitting of reflectivity data from the water-FAS25 SAM interface (the experimental data are in Fig. 3). (a) Best-fit density profile (dashed line shows the slabs without interface rounding); (b) merit function landscape in the D_{gap}-ρ_{gap} plane when all other parameters are fixed at the best-fit values; (c) merit function landscape when all other parameters are allowed to float. Note that in (c) the axis extends to negative values, indicating the possibility of an "inverse gap" with density larger than water. The merit function γ^2 [Eq. (3)] is shown with its best value ${\gamma_{\text{min}}}^2$ subtracted and then scaled by a factor of 1000. The visible color range is from $\gamma^2 = {\gamma_{\text{min}}}^2$ (dark) to $\gamma^2 = 1.50{\gamma_{\text{min}}}^2$ (light).

These results illustrate that increasing the total number of variable parameters reduces the precision with which the parameters of interest can be determined. This should not obscure the crucial result: even under the harsh conditions where all parameters are allowed to float [Fig. 4(c)], there is no ambiguity regarding the existence of a gap (with $\rho_{\text{gap}} < \rho_{\text{water}}$, $D_{\text{gap}} > 0$) at the FAS25-water interface. While our more detailed analysis increases the uncertainties in the

quantitative values of the gap parameters, it increases our level of confidence in the qualitative conclusion that a gap exists.

Figure 5 shows contours similar to those in Fig. 4(c) but for the other SAMs studied (FAS13, FAS17, and FAS21). In the case of FAS13, the shortest chain molecule, it can be seen that the points along the vertical line $D_{gap} = 0$ and on both sides of the horizontal line $\rho_{gap} = \rho_{water}$ would also give quite good fits. Since this means that the gap can be normal, inverted, or nonexistent, we must conclude that there is no evidence of a gap between our FAS13 SAMs and water. In the case of FAS17, again, there are good fits along the vertical line $D_{gap} = 0$ and on both sides of the vertical line $\rho_{gap} = \rho_{water}$. However, for FAS21 (just as with FAS25, shown earlier), the contours exclude the possibility of zero or inverted gaps. There is a normal gap ($\rho_{gap} < \rho_{water}$, $D_{gap} > 0$).

IV. DISCUSSION

The results above help explain why different groups studying apparently similar systems have reported significantly different results. Statistical variations in the data, the use of various merit functions, and the use of different software algorithms can determine which of many essentially degenerate points are arbitrarily selected as giving the best fit. Contours such as those we have shown give the bigger picture.

The interface of FAS17 monolayers with water has also been studied by another group using x-ray reflectivity.[52] Our FAS17 raw data (Fig. 3) are almost identical to the data reported in Ref. 52. They report gap parameters corresponding to $D_{gap} = 3.2$ Å and $(\rho_{water} - \rho_{gap})/\rho_{water} = 0.44$. As we have shown, the gap width and density cannot really be determined to this level of accuracy; however, their reported parameters fall within the colored region of our FAS17 contour (Fig. 5). Note also that they used silicon with native oxide and assumed an impossibly small Si-SiO_2 interface width (0.2 Å). Such an interface would generate a strong reflectivity minimum on its own (matching the second minimum in the data). The fact that our reflectivity data (using thermal oxide) are essentially identical to those in Ref. 52 (using native oxide) proves that such an ultrasharp oxide interface does not exist in reality.

Our results are also consistent with a recent study[53] of the interface between water and epitaxial graphene grown on SiC substrates. In this experiment, the crystal truncation rods of the substrate were measured, which allowed the gap width to be determined with much higher resolution than is possible with the specular reflectivity technique. They reported a 0.2-Å-wide gap, but since the graphene surface is not very hydrophobic (contact angle 93°), the authors note that their results are "consistent with the idea of a gap whose magnitude is a function of the contact angle" Ref. 53 (p. 035406).

Nonetheless, while contact angle measurements are easy and intuitive, their relevance is unclear in general. For example, Ref. 52 (p. 6735) notes that "the complex interplay between surface chemistry and topography precludes the existence of a direct and universal relation between the macroscopic contact angle and the nanoscopic water depletion." This is a reasonable concern; to put it another way, the contact angle is a nonequilibrium measurement (the advancing and receding angles are different) and depends on surface defects that vary from sample to sample but are not relevant to the average gap width. We have therefore sought to identify a different explanation for why the gap differs so much from one SAM to another.

The different SAMs we studied obviously have different thicknesses, and the distance from water to the oxide layer could affect the gap. We see unambiguous gaps only with our longer chain SAMs (FAS21 and FAS25). On the other hand, monolayer self-assembly is known to be subject to significant irreproducibility, and that the shortest chain monolayer (FAS13) also has the lowest chain density (Tables I and II), indicating poor lateral packing during SAM deposition. FAS21, which has the highest chain density but not the largest chain length, shows the best-defined contours and an unambiguous gap. Hence, one possibility is that the gap depends on the monolayer density.

In Fig. 6 we have plotted the chain slab density from our fits, ρ_c, against the effective gap parameter D_{eq} [see Eq. (3)]. Rather than reporting the range of D_{eq} along the "bottom of the valley"; i.e., only for the points with the best merit function, we have included in Fig. 6 the much larger ranges of D_{eq}, covering the entire colored region in each contour (i.e., including all fits where the merit functions are anywhere between the best-fit value ${\gamma_{min}}^2$ and 50% above that value). It can be seen that even with this very conservative criterion, FAS21 and FAS25 have positive definite D_{eq} (normal gaps). Indeed, since

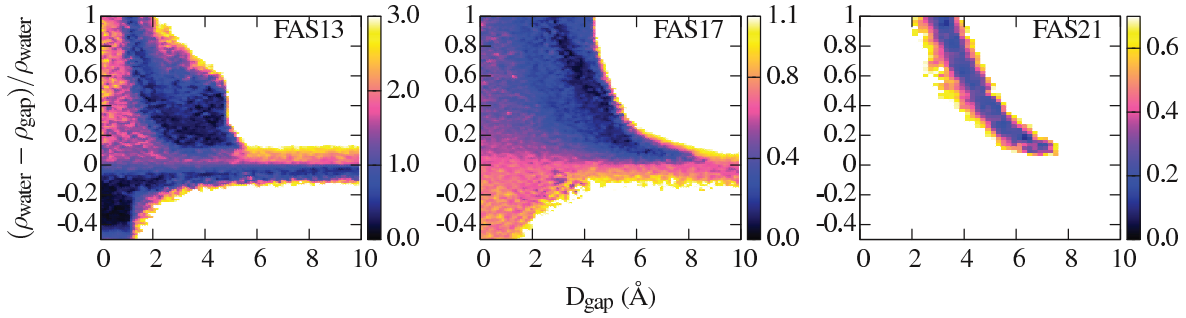

FIG. 5. (Color online) Merit function landscapes in the D_{gap}-ρ_{gap} plane for fitting of reflectivity data from water-FAS13/FAS17/FAS21 interfaces (the experimental data are in Fig. 3). All other parameters were allowed to float. Note that the y axes extend to negative values, allowing for "inverted gaps" with density larger than water. The merit function γ^2 [Eq. (3)] is shown with its best value ${\gamma_{min}}^2$ subtracted and then scaled by a factor of 1000. The visible color range is from $\gamma^2 = {\gamma_{min}}^2$ (dark) to $\gamma^2 = 1.50{\gamma_{min}}^2$ (light).

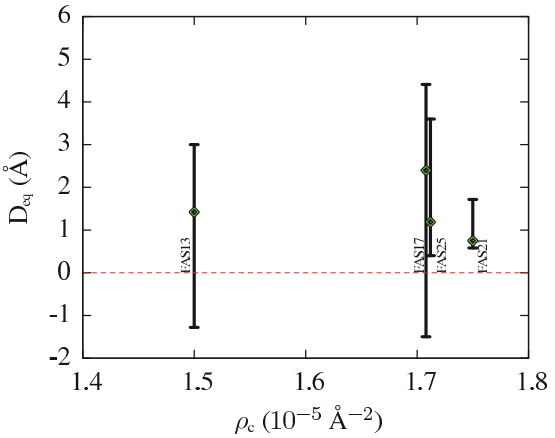

FIG. 6. (Color online) Effective gap width D_{eq} [Eq. (4)] vs SAM chain density ρ_c (from dry SAM fits) for the four SAMs studied. The points show the D_{eq} values for the best possible fits (as discussed in the text, there are many almost degenerate fits). The error bars show the D_{eq} range corresponding to the merit function ranging from its minimum value to 50% above that value. It can be seen that the two higher density, longer chain SAMs have $D_{eq} > 0$ (positive definite gap).

better packed SAMs should also be more hydrophobic, our results are consistent with the qualitative expectation that more hydrophobic SAMs will have larger gaps.

V. CONCLUSIONS

X-ray reflectivity is a powerful nondestructive characterization technique with high spatial resolution. The analysis in this paper explains why the water-hydrophobic interface has been a far more difficult challenge for this technique than expected and why there has been so much disagreement and debate. There are undoubtedly some systems where the merit function landscape has a simple, idealized form, leading to precise measurements of relevant parameters, but this is not one of them. Previous studies, including our own, have oversimplified the problem by not fully accounting for the complexity of the landscape and by allowing software to choose a best fit when many nearly degenerate fits are available.

Our more detailed analysis using very conservative criteria results in less precise numerical estimates, but the overall picture emerges more clearly. Our results provide confirmation for the gap hypothesis, and we suggest that they can serve as a reality check on the results of computer simulations. Models that are consistent with these experimental results are more realistic and will be better able to predict other aspects of the behavior of water near interfaces.

ACKNOWLEDGMENTS

This work was supported by the US National Science Foundation under Grant No. DMR-1006432. We thank Evguenia A. Karapetrova for her help in synchrotron experiments and Jangdae Youn for his contribution to the early stages of this project. We used the X-Ray Opera-tions and Research Beamline 33-BM-C at the Advanced Photon Source, Argonne National Laboratory. Use of the Advanced Photon Source, an Office of Science User Facility operated for the US Department of Energy (DOE) Office of Science by Argonne National Laboratory, was supported by the US DOE under Contract No. DE-AC02-06CH11357.

*Present address: Chemical Sciences and Engineering Division, Argonne National Laboratory, Argonne, Illinois 60439, USA.
†Present address: Advanced Photon Source, Argonne National Laboratory, Argonne, Illinois 60439, USA.

[1]F. H. Stillinger, J. Solution Chem. **2**, 141 (1973).
[2]D. Chandler, Nature (London) **437**, 640 (2005).
[3]M. Maccarini, Biointerphases **2**, MR1 (2007).
[4]F. Sedlmeier, J. Janecek, C. Sendner, L. Bocquet, R. R. Netz, and D. Horinek, Biointerphases **3**, FC23 (2008).
[5]P. G. de Gennes, Langmuir **18**, 3413 (2002).
[6]L. Lurio, T. Rabedeau, P. Pershan, I. F. Silvera, M. Deutsch, S. Kosowsky, and B. Ocko, Phys. Rev. Lett. **68**, 2628 (1992).
[7]B. Ocko, X. Wu, E. Sirota, S. Sinha, and M. Deutsch, Phys. Rev. Lett. **72**, 242 (1994).
[8]M. K. Sanyal, S. K. Sinha, K. G. Huang, and B. M. Ocko, Phys. Rev. Lett. **66**, 628 (1991).
[9]W. Zhao, X. Zhao, J. Sokolov, M. Rafailovich, M. K. Sanyal, S. K. Sinha, B. H. Cao, M. W. Kim, and B. B. Sauer, J. Chem. Phys. **97**, 8536 (1992).
[10]W. Zhao, M. Rafailovich, J. Sokolov, L. Fetters, R. Plano, M. Sanyal, S. Sinha, and B. Sauer, Phys. Rev. Lett. **70**, 1453 (1993).
[11]O. Magnussen, B. Ocko, M. Regan, K. Penanen, P. Pershan, and M. Deutsch, Phys. Rev. Lett. **74**, 4444 (1995).
[12]O. Shpyrko, P. Huber, A. Grigoriev, P. Pershan, B. Ocko, H. Tostmann, and M. Deutsch, Phys. Rev. B **67**, 115405 (2003).
[13]E. DiMasi, H. Tostmann, O. G. Shpyrko, M. Deutsch, P. S. Pershan, and B. Ocko, J. Phys.: Condens. Matter **12**, A209 (2000).
[14]M. Regan, E. Kawamoto, S. Lee, P. Pershan, N. Maskil, M. Deutsch, O. Magnussen, B. M. Ocko, and L. Berman, Phys. Rev. Lett. **75**, 2498 (1995).
[15]H. Tostmann, E. DiMasi, P. S. Pershan, B. M. Ocko, O. G. Shpyrko, and M. Deutsch, Phys. Rev. B **59**, 783 (1999).
[16]O. G. Shpyrko, A. Y. Grigoriev, C. Steimer, P. S. Pershan, B. Lin, M. Meron, T. Graber, J. Gerbhardt, B. M. Ocko, and M. Deutsch, Phys. Rev. B **70**, 224206 (2004).
[17]B. Yang, D. Gidalevitz, D. Li, Z. Huang, and S. A. Rice, Proc. Natl. Acad. Sci. USA **96**, 13009 (1999).
[18]B. Yang, D. Li, Z. Huang, and S. A. Rice, Phys. Rev. B **62**, 13111 (2000).
[19]B. Yang, D. Li, and S. A. Rice, Phys. Rev. B **67**, 212103 (2003).
[20]H. Mo, G. Evmenenko, S. Kewalramani, K. Kim, S. N. Ehrlich, and P. Dutta, Phys. Rev. Lett. **96**, 096107 (2006).
[21]H. Mo, S. Kewalramani, G. Evmenenko, K. Kim, S. N. Ehrlich, and P. Dutta, Phys. Rev. B **76**, 024206 (2007).
[22]A. Braslau, M. Deutsch, P. S. Pershan, A. H. Weiss, J. Als-Nielsen, and J. Bohr, Phys. Rev. Lett. **54**, 114 (1985).

[23]S. Chattopadhyay, A. Uysal, B. Stripe, S. Ehrlich, E. A. Karapetrova, and P. Dutta, Phys. Rev. B **81**, 184206 (2010).
[24]S. Chattopadhyay, A. Uysal, B. Stripe, G. Evmenenko, S. Ehrlich, E. A. Karapetrova, and P. Dutta, Phys. Rev. Lett. **103**, 175701 (2009).
[25]O. Shpyrko, M. Fukuto, P. Pershan, B. Ocko, I. Kuzmenko, T. Gog, and M. Deutsch, Phys. Rev. B **69**, 245423 (2004).
[26]C.-J. Yu, A. G. Richter, A. Datta, M. K. Durbin, and P. Dutta, Phys. Rev. Lett. **82**, 2326 (1999).
[27]C. J. Yu, A. G. Richter, J. Kmetko, S. W. Dugan, A. Datta and P. Dutta, Phys. Rev. E **63**, 021205 (2001).
[28]C. J. Yu, G. Evmenenko, J. Kmetko, and P. Dutta, Langmuir **19**, 1053 (2003).
[29]B. Hou, N. Lanaait, H. Yu, W. Boo, J. Yun, B. Lin, M. Meron, G. Luo, P. Vanysek and M. L. Schlossman, J. Phys. Chem. B **117**, 5365 (2013).
[30]K. Kashimoto, J. Yoon, B. Hou, C. H. Chen, B. Lin, M. Aratono, T. Takiue, and M. L. Schlossman, Phys. Rev. Lett. **101**, 076102 (2008).
[31]D. Schwendel, T. Hayashi, R. Dahint, A. Pertsin, M. Grunze, R. Steitz, and F. Schreiber, Langmuir **19**, 2284 (2003).
[32]R. Steitz, T. Gutberlet, T. Hauss, B. Klösgen, R. Krastev, S. Schemmel, A. C. Simonsen, and G. H. Findenegg, Langmuir **19**, 2409 (2003).
[33]D. A. Doshi, E. B. Watkins, J. N. Israelachvili, and J. Majewski, Proc. Natl. Acad. Sci. USA **102**, 9458 (2005).
[34]Y. S. Seo and S. Satija, Langmuir **22**, 7113 (2006).
[35]A. Poynor, L. Hong, I. K. Robinson, S. Granick, Z. Zhang, and P. A. Fenter, Phys. Rev. Lett. **97**, 266101 (2006).
[36]M. Mezger, H. Reichert, S. Schöder, J. Okasinski, H. Schröder, H. Dosch, D. Palms, J. Ralston, and V. Honkimäki, Proc. Natl. Acad. Sci.USA **103**, 18401 (2006).
[37]M. Maccarini, R. Steitz, M. Himmelhaus, J. Fick, S. Tatur, M. Wolff, M. Grunze, J. Janecek, and R. Netz, Langmuir **23**, 598 (2007).
[38]P. A. Fenter, Rev. Mineral. Geochem. **49**, 149 (2002).
[39]S. Chattopadhyay, A. Uysal, B. Stripe, Y.-g. Ha, T. J. Marks, E. A. Karapetrova, and P. Dutta, Phys. Rev. Lett. **105**, 037803 (2010).
[40]B. B. Luokkala, S. Garoff, and R. M. Suter, Phys. Rev. E **62**, 2405 (2000).
[41]K. Paso, R. M. L. Helberg, S. Raaen, and J. Sjöblom, J. Colloid Interface Sci. **325**, 228 (2008).
[42]S. K. Sinha, E. B. Sirota, S. Garoff, and H. B. Stanley, Phys. Rev. B **38**, 2297 (1988).
[43]L. G. Parratt, Phys. Rev. **95**, 359 (1954).
[44]A. Nelson, J. Appl. Crystallogr. **39**, 273 (2006).
[45]S. M. Danauskas, D. Li, M. Meron, B. Lin and K. Y. C. Lee, J. Appl. Crystallogr. **41**, 1187 (2008).
[46]S. Kirkpatrick and M. Vecchi, Science **220**, 671 (1983).
[47]C. F. Laub and T. L. Kuhl, J. Chem. Phys. **125**, 244702 (2006).
[48]R. C. Aster, B. Borchers, and C. H. Thurber, *Parameter Estimation and Inverse Problems*, 2nd ed. (Academic Press, Waltham, MA, 2012).
[49]M. Mezger, H. Reichert, B. M. Ocko, J. Daillant, and H. Dosch, Phys. Rev. Lett. **107**, 249801 (2011).
[50]S. Chattopadhyay, A. Uysal, B. Stripe, Y.-g. Ha, T. J. Marks, E. A. Karapetrova, and P. Dutta, Phys. Rev. Lett. **107**, 249802 (2011).
[51]Xidong Chen and J. M. Gibson, J. Vac. Sci. Technol. A **17**, 1269 (1999).
[52]M. Mezger, F. Sedlmeier, D. Horinek, H. Reichert, D. Pontoni, and H. Dosch, J. Am. Chem. Soc. **132**, 6735 (2010).
[53]H. Zhou, P. Ganesh, V. Presser, M. C. F. Wander, P. Fenter, P. R. C. Kent, D.-e. Jiang, A. A. Chialvo, J. McDonough, K. L. Shuford, and Y. Gogotsi, Phys. Rev. B **85**, 035406 (2012).